International Journal Of Engineering Research And Development
e- ISSN: 2278-067X, p-ISSN: 2278-800X, www.ijerd.com
Volume 21, Issue 1 (January, 2025), PP 92-101

Computational Analysis of Urine & Kidney Stone in Renal Ureter

Haider Ali[1], Saad Shakir[2], Fawad Ahmad[2], Jibran Bin Hussain[2],
[1]*Department of Mechanical Engineering,*
University of Engineering and Technology Peshawar, Pakistan
[2]*Department of Mechanical Engineering,*
CECOS University of IT & Emerging Sciences, Peshawar, Pakistan

ABSTRACT
Peristalsis in the ureter accelerates flow of urine between the kidney and the bladder. Sometimes, flow of urine is accompanied by solid masses of highly concentrated minerals (calcium, sodium, uric acid, phosphate etc.) in the ureter. Thus, effecting operation of the urine flow and cause severe discomfort. Kidney stones can vary in size and shape which significantly impact their treatment procedures and potential complication.
In this research, the peristalsis of the ureter with and without stone is modelled by axisymmetric two-dimensional computational fluid dynamics simulations using the commercial package ANSYS FLUENT. The peristalsis is modelled as sinusoidal wave with a particular physiological velocity. The study examines flow in the ureter with peristalsis in the absence of any blockage. The second section of the study evaluates the effects of different obstructions (30, 50 and 70%) for round shaped stones of multiple sizes. The third section of study evaluates the effect of stone shape. To illustrate backflow, trapping, and reflux phenomena and to keep an eye on the condition of the ureteral wall in the event of an obstruction, pressure contours, velocity vectors, profiles of pressure gradient magnitudes, and wall shear stresses are displayed along one bolus of the ureteral wall.
The result has revealed that pressure gradient and wall shear stress were higher during contraction of peristaltic wave. Peak Trapping phenomena was noticed at start of ureter for highest obstruction case. Moreover, ureter wall contraction was the reason for the backflow of urine in the presence of stone and without stone.

Date of Submission: 02-01-2025 Date of acceptance: 13-01-2025

I. INTRODUCTION

The urinary system is made up of a group of organs in the body which will discharge excess fluids and other substances out from the bloodstreams.[1] During the process of excretion, the clear particles are absorbed by the bloodstreams while unfiltered particles (mineral) make their path from the kidney to ureter, then to bladder and finally expelled out of the body through urethra. Many minerals including calcium, sodium, potassium, oxalate, uric acid, and phosphate are found in urine. These mineral deposits build up inside the upper urinary system and form kidney stones. Growth of mineral deposits into visible stone have various time periods which is based on reaction state.[2] Kidney stones come in various sizes and it can significantly impact their treatment and potential complications. They can vary in size from being as small as a grain of sand to as large as a golf ball. The size of a kidney stone is a crucial factor in determining the appropriate treatment approach. Small stones less than 4 mm can often pass through the urinary tract without medical intervention. They may cause discomfort or pain during urination but are usually manageable with increased fluid intake and pain medication. Medium-sized stones range from 4-6 mm may or may not pass on their own. Some individuals may require medical intervention, such as medications to help relax the muscles of the ureter or procedures like lithotripsy to break up the stone to facilitate passage Stones larger than 6 mm often require medical intervention for removal. Options may include procedures such as ureteroscopy, percutaneous nephrolithotomy, or occasionally open surgery in rare and severe cases. Round and smooth stones may pass more easily through the urinary tract since they are less likely to get lodged in the ureter. However, even round stones can cause significant discomfort and pain during passage. Irregular and jagged stones with irregular shapes may have rough edges, increasing the likelihood of getting stuck in the urinary tract. These stones can cause more severe pain and may require more invasive treatment methods for removal. Staghorn type of kidney stone that fills a large portion of the kidney's renal pelvis. Staghorn stones can be challenging to treat and often require surgical intervention due to their size and shape. Lack of awareness regarding kidney stones can have a significant negative impact on health care resources. Various risk factors include eating poorly, consuming insufficient

amounts of water, and having coexisting conditions such as diabetes, hypertension, dyslipidemia, obesity, coronary artery disease, and depression [3].

Over the past 20 years, there has been an increase in the occurrence of kidney stone disease, with a growing burden of disease across age, gender, and race. Based on available data, kidney stone disease is estimated to affect about 16% of Pakistanis. Age-specific occurrence of urolithiasis ranges from 12.2% in 20-29 year-olds to 31.5% in 40-49 year-olds and 29.6% in 30-39 year-olds [4,5]. When a stone becomes large enough to graze the urinary system walls, it can lead to bleeding, infection, urine backflow, and kidney injury. Moreover, these stones can cause severe discomfort and high renal pressures because they frequently become trapped and obstruct the path of urine flow in renal ureter of kidney system. As a result, there are burning sensations during urination and symptoms of nausea and vomiting. There are various remedial procedures for urinary tract stones depending on their size and location. However, problems like mucosal damage, false passage, ureteral perforation, ureteral rupture, stricture, incapacity to remove the device, and ureteral avulsion might occasionally result from these treatments. These issues may result in longer operating room stays and higher costs, and in certain situations, they may have catastrophic and long-lasting effects.

The goal of this research is to study the influence of stone size and shape on urine flow in the availability of muscle contraction peristalsis mechanism. ANSYS Fluent was used to examine the impact of various stone shapes (round, hexagon & star) and sizes (3mm, 5mm & 7mm) on the urine flow in the renal ureter and the ureteral wall shear stress. Based on the impact of the calculi on the renal ureteral wall and urine flow in the renal ureter, the in-depth analysis and study can aid in improving our knowledge of the behaviour of a clogged renal ureter and may result in improved patient outcomes and stone treatment.

II. NUMERICAL SETUP

INPUT PARAMETER

The urine is considered to be a viscous, homogenous, incompressible Newtonian fluid with a density of 1050 kg/m3, and a viscosity of $\mu = 1.3$ cP at 298 K. The Reynolds number calculated as $Re = \rho UL/\mu$ is 1.72 and thereby laminar flow is considered. The transient analysis has been carried out with time step size of 0.01 and total number of time step were 800. The duration of non-steady and transient analysis is 8 seconds. To obtain correct results, the convergence requirement of 10-6 per time step is defined for each of the governing equations to make sure satisfactory convergence. The pressure-velocity coupling strategy was implemented using the SIMPLE (Semi-Implicit approach for pressure-linked equations) scheme. The method of discretizing gradients was based on the least squares cell approach. For dynamic mesh, diffusion-based smoothing and unified remeshing was considered. The user defined function was compiled using in-built compiler and loaded to ANSYS Fluent library. The ureter wall is chosen for dynamic mesh zone where mesh motion is generated. A standard scheme was utilised to determine the pressures, and the second-order upwind strategy was employed to calculate the flow momentum.

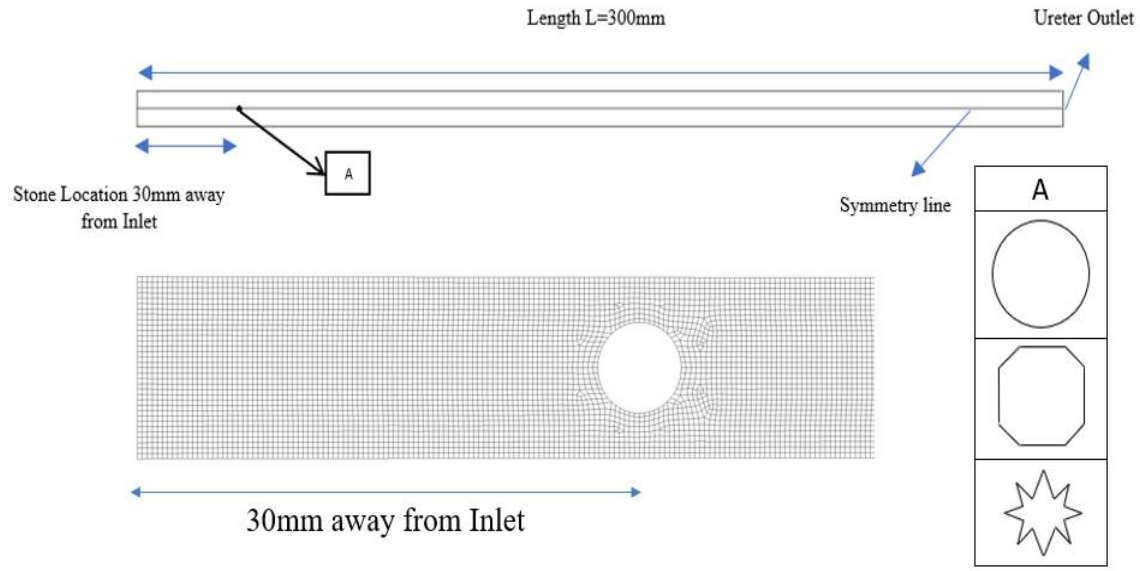

Figure 1: Dimension of fluid domain, Finite Element Model, Shapes of Kidney Stone

FINITE ELEMENT MODEL

To ensure that the numerical results are independent of the size of the mesh elements, mesh convergence analyses were performed to examine flow input variables with coarser (nine thousand) and finer

(twenty-seven thousand) mesh size. The independence test of time step size was also conducted for various distinct step sizes, namely 0.001, 0.01, and 0.05 s. For the mesh and time step dependent study, the percentage errors were found to be fewer than 0.7 and 1%, respectively. Therefore, 17,000 structural quadrilateral type elements with size of 0.3mm was used to mesh the fluid domain and solution was ran for 800 total time steps with time step size of 0.01.

FLUID FLOW

The continuity and momentum equations are the governing equations used to compute the fluid flow:

$$\frac{1}{x}\frac{\partial(xv_x)}{\partial x} + \frac{\partial(v_y)}{\partial y} = 0 \quad Equation\ (1)$$

$$\rho\left(\frac{\partial v_x}{\partial t} + v_x\frac{\partial v_x}{\partial x} + v_y\frac{\partial v_x}{\partial y}\right) = -\frac{\partial P}{\partial x} + \mu\left[\frac{1}{x}\frac{\partial}{\partial x}\left(x\frac{\partial v_x}{\partial x}\right) - \frac{v_x}{x^2} + \frac{\partial^2 v_x}{\partial y^2}\right] \quad Equation\ (2)$$

$$\rho\left(\frac{\partial v_y}{\partial t} + V_x\frac{\partial v_y}{\partial x} + v_y\frac{\partial v_y}{\partial y}\right) = -\frac{\partial P}{\partial y} + \mu\left[\frac{1}{x}\frac{\partial}{\partial x}\left(x\frac{\partial v_y}{\partial x}\right) + \frac{\partial^2 v_y}{\partial y^2}\right] \quad Equation\ (3)$$

Where ρ and P represent density and pressure respectively; μ represents dynamic viscosity of the fluid; and v_x and v_y signify velocity of fluid in x and y direction respectively.

WALL SHEAR STRESS

Wall shear stress represents the frictional force experienced by the inner lining of the ureter due to the flow of urine passing through it. The force is parallel to the direction of flow and is influenced by factors such as fluid viscosity, flow rate, and the geometry of the ureter. High wall shear stress can indicate increased irregularities in urine flow, which may have implications for conditions like urinary tract obstructions or kidney stones. Wall shear stresses are computed as below:

$$\tau = \mu\left(\frac{\partial v_x}{\partial y} + \frac{\partial v_y}{\partial x}\right) Equation\ (4)$$

Where τ is wall shear stress, μ is dynamic viscosity of 1.3 cP, $\frac{\partial v_x}{\partial y}$ and $\frac{\partial v_y}{\partial x}$ are velocity gradient in respective directions.

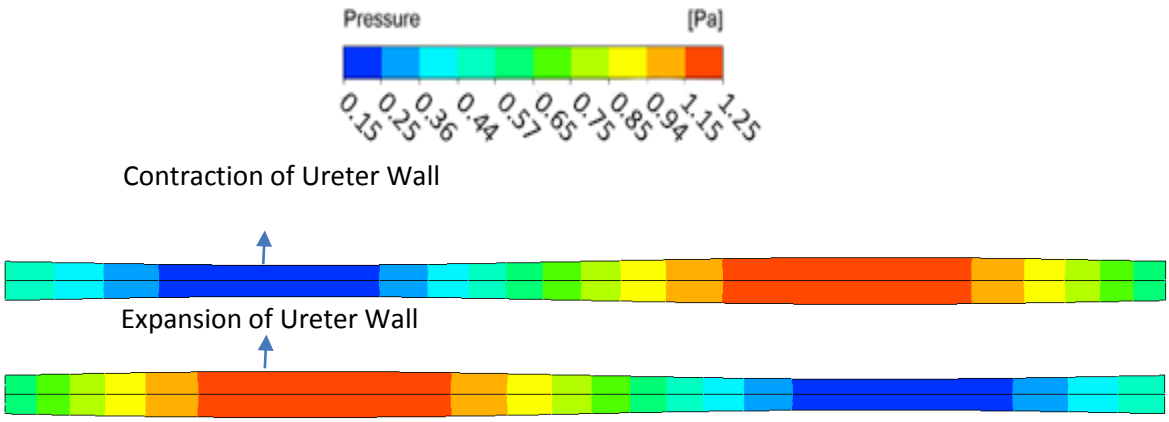

Figure 2: Peristalsis Muscle contraction and expansion in Renal Ureter

BOUNDARY CONDITIONS

- No slip between ureter wall surface and urine is considered because when a urine flows over a ureter wall surface, the urine molecules are in direct contact with the surface experience a force from the wall that prevents them from slipping past it. Instead, they adhere to the surface and move with the same velocity as the surface itself. At the molecular level, the urine molecules interact with the solid surface of ureter wall through intermolecular forces, such as electrostatic forces. These forces cause the fluid molecules to adhere to the surface. The adherence of fluid molecules to the solid surface is a result of viscosity, the resistance of a fluid to shear deformation. Viscosity is a property that determines how easily adjacent fluid layers slide past each other.
- The constant pressure difference of 0.3Pa has been applied across the fluid domain to provide driving force required to maintain the flow of urine from the kidneys to the bladder, facilitated by peristalsis.
- The symmetric boundary condition is applied at the symmetry plane of ureter. The urine flow is laminar and fluid domain has uniform cross section. Instead of modeling the entire flow domain, only one portion of the

flow domain is simulated. Applying the symmetry boundary condition, the computational domain can be reduced in size, which has significantly reduced the computational cost of simulations. Moreover, it has reduced the time period required for each simulation.

III. RESULT AND DISCUSSION

This work presents and analyses a numerical model of urine flow in the renal ureter containing and without calculi cases. Kidney calculi of numerous sizes are placed into the renal ureter, and the displacement per unit time vector magnitude, change in pressure per unit length and wall shear stresses between the various situations are analysed to determine the consequence of the blockage on the flow of urine dynamics and the renal ureter wall.

PERISTALTIC WAVE WITHOUT ANY OBSTRUCTION:

The examination of the muscle contraction peristalsis mechanism in an empty ureter is presented in the first section of the paper. Figure 2 displays pressure contours at two distinct moments, which correspond to contraction and expansion of the peristalsis wave. As was already indicated, there is a constant pressure difference of 0.3 Pa between the inlet and the output. This persistent pressure variation, which changes evenly between the ends, results in a consistent flow between the ureter inlet and outlet, regardless of peristaltic movement However, due to the wall's added peristaltic motion, pressure fluctuation is not anymore linear, and

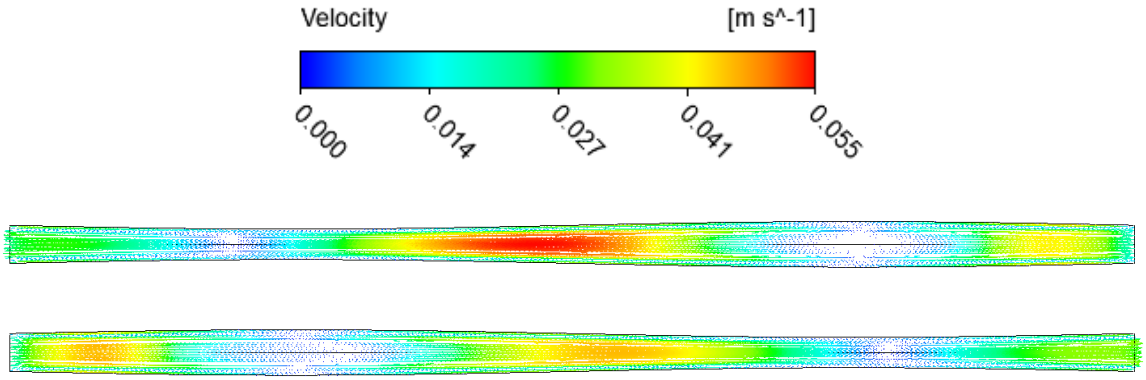

Figure 3: Peristalsis muscle contraction mechanism and recirculation phenomena in the Renal Ureter.

flow is nonlinear. In each of the two examples, high-pressure zones occur after the contractions. Additionally, there is a negative pressure gradient near the intake at contraction of peristaltic wave, right after the first contraction. This pressure gradient continues downstream to the center of the ureter. High pressure gradients tend to reverse or create a flow that is opposite to the motion of the peristaltic wave, as well as generate recirculation.

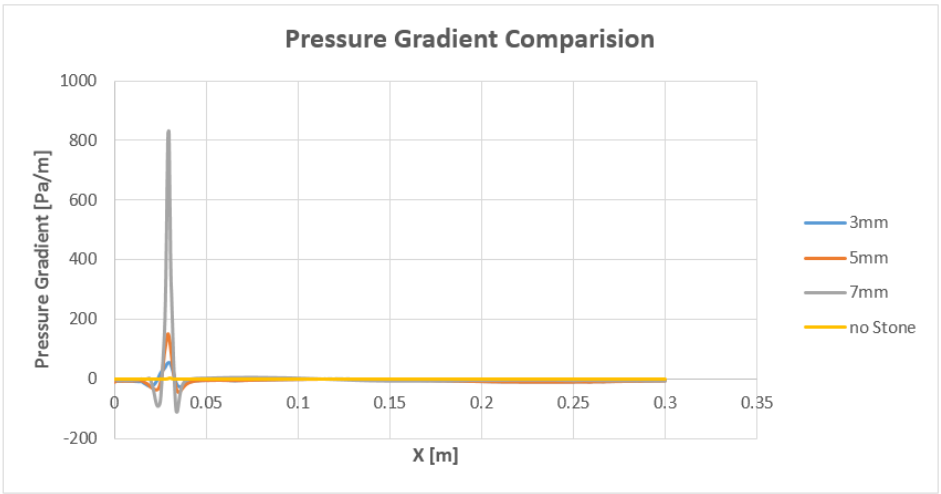

Figure 4: Comparison of Pressure Gradient for round shaped stone with various sizes (3,5 and 7mm).

Fluid velocity vectors can be used to confirm this. The change in displacement per unit time vectors are displayed in Figure 3 following a muscle contraction mechanism of peristalsis movement, flow of urine in reverse direction was observed at the renal ureter's start, as well as regular deceleration spots where urine reversed to its nearby section. The flow's inertia causes an unfavourable pressure gradient, which is the cause of the backflow. The findings show that the velocity of urine peaks shortly after contraction, around the midline and resulting in a high-velocity jet flow. The fact that there are going to be areas with restricted streams and fluid backflow is a crucial aspect of peristaltic motion. The streamlines and velocity vectors of the peristaltic movement are displayed in Figure 5.1. The streamlines are sealed at various points throughout the two-time occurrences displayed, According to Vahidi et al., this phenomenon is referred to as entrapment and is a feature of the pumping motion. It is important to remember that the flow is constant in a dynamic reference coordinate, hence the axial pressure gradient, dp/dz, can be used to describe the pumping performance. At the moments of contraction of the peristaltic movement, the change in pressure per unit length across the renal ureter center line were computed and are displayed as a single-valued dependent variable of the center line dimension in Figure 4.

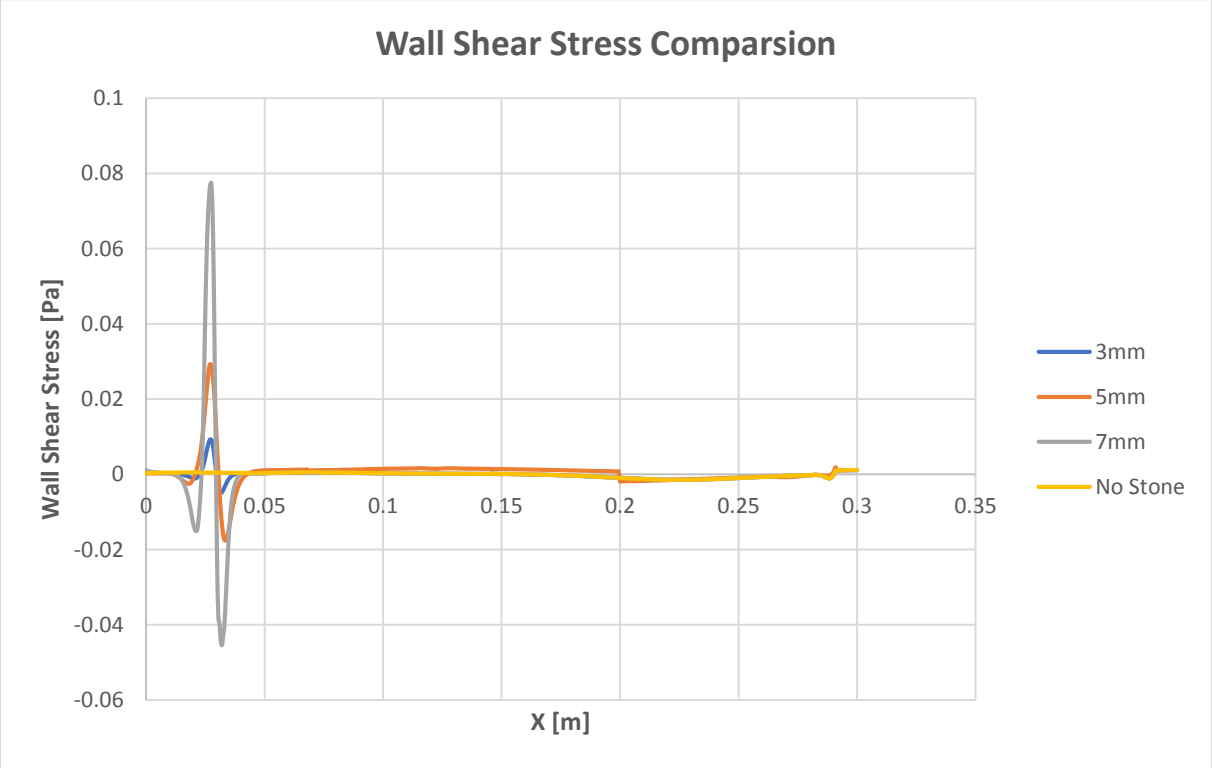

Figure 5: Comparison of Wall Shear Stress for round shaped stone with various sizes (3,5 and 7mm).

The results revealed that the pressure gradient for no stone case where intensity along the renal ureteral axis on its center line was maximum during the shrinkage stages and thereafter reduced downstream due to the advantageous force per unit area boundary scenario. But compared to other stone with larger in diameter, the change in pressure per unit length curve is almost linear. This is due to the fact that magnitude of pressure gradient for other stone are very high for obstructed case. However, the residual effects of the earlier peristaltic motion, the pressure gradient does fluctuate throughout the stages of the ureter that are straight. It is evident that pressure gradient increases with the increase in stone size. Greater local pressure gradients were produced by the ureter's contraction as opposed to the straight stages. The wall's shear stresses were computed for various stone sizes. The wall shear stress of peristalsis wave is shown in Figure 5. The wall shear stress for no stone case is displaced. There is fluctuation in wall shear stress but it is negligible compare to other stone cases plus it is normal. The fluctuation in wall shear stress is caused by stretching in wall due to peristalsis muscle contraction in ureter. Moreover, the force exerted by the urine on round 7mm stone is also calculated using ANSYS Fluent. It is calculated by utilizing drag force formula and stated as 7.88×10^{-6} N. The combination of ureter peristalsis wave and pressure difference across the ureter is require to push the urine to produce at least 7.88×10^{-6} N of force at the surface of stone to push the it in the direction of fluid flow.

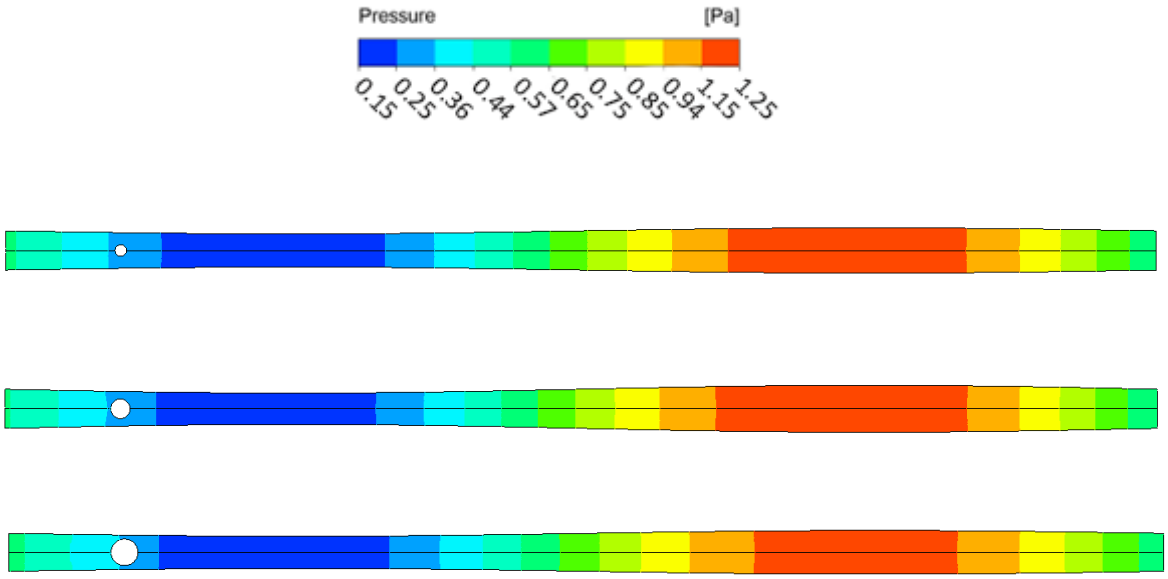

Figure 6: Pressure Contours for round shaped stone with various sizes (3, 5 and 7mm).

PERISTALTIC WAVE WITH ROUND SHAPED STONE:

In this section of study the shape of stone is considered round and the muscle contraction peristalsis wave mathematical model was computed for the ureter with varying stone sizes. Comparisons are drawn between the ureter with the muscle contraction peristalsis wave with obstruction and the various diameters, which replicate various real-life scenario. The contours for various blockages in ureter for pressure are displayed in Figure 6, for 30, 50, and 70% obstructions. Following the contraction wave, a high-pressure gradient is visible. This gradient increases with obstruction and is noticeably greater in the 70% ureteral blockage example. For every scenario shown, the change in displacement per unit time vectors colored by the displacement per unit time magnitude in m/s were displayed at time when muscle contraction peristalsis was at peak. Three distinct insets highlight and explain the flow patterns across the ureter in the presence of peristalsis muscle contraction wave. As the volume of the stone grows, the backflow adjacent to the calculi also increases. This is due to an growth in the hydrostatic pressure near obstacle and cause urine to backflow. Because of the greatest blockage, the 70% ureteral obstruction case had the greatest reverse velocities at the inlet and a substantial reverse flow at the start of ureter compared to all other scenarios. Zones with urine flow in reverse direction form in the various sections of the ureter as a result of the peristaltic action, and as obstruction increases, the fluid velocities in the ureter distal to the stone decrease. For the ureter in each of the various obstruction scenarios, the magnitude of pressure gradient through the symmetry axis was examined and plotted. This magnitude of pressure gradient during the wall shrinkage under peristalsis are depicted in Figure 4. Pressure gradient "spikes" were caused by the stone's presence and peaked for the 70% blockage scenario. As the obstruction percentage increased, these "spikes" increased. Thus, the tiniest stone had the lowest pressure gradient magnitude. This is most likely due to the fact that as the obstruction grows, the fluid becomes more obstructed, which lowers both the pressure within the obstruction and pressure change increases occurring across it. Equation (4) was used to compute the magnitude of wall shear stresses in the presence of peristalsis wave of obstructed ureter. The results are displayed for the various obstructions in Figure 5. The stone alters the behaviour of the wall shear stress. At the stone's placement, the wall shear stress increases noticeably before returning to its normal level. Keep in mind that the usual values pertain to the ureter's values when there is no stone present. Furthermore, the magnitude is raised by nearly 3 times in the 70% ureteral obstruction case relative to the normal unobstructed condition of ureter. As the obstruction grows larger, the wall shear stress climbs to its peak value during contraction. This is fact due to the fluid fraction force increases as the obstruction volume increase. Thus, increasing the magnitude of wall shear stress and create high index pain.

PERISTALTIC WAVE WITH DIFFERENT SHAPE STONES:

In this section of study, the size of stone is considered 7mm i.e. 70% obstruction and the muscle contraction peristalsis wave mathematical model was computed for various shapes of stone (round, hexagon and

star). Comparisons are drawn between the ureter with the muscle contraction peristalsis wave with obstruction and the

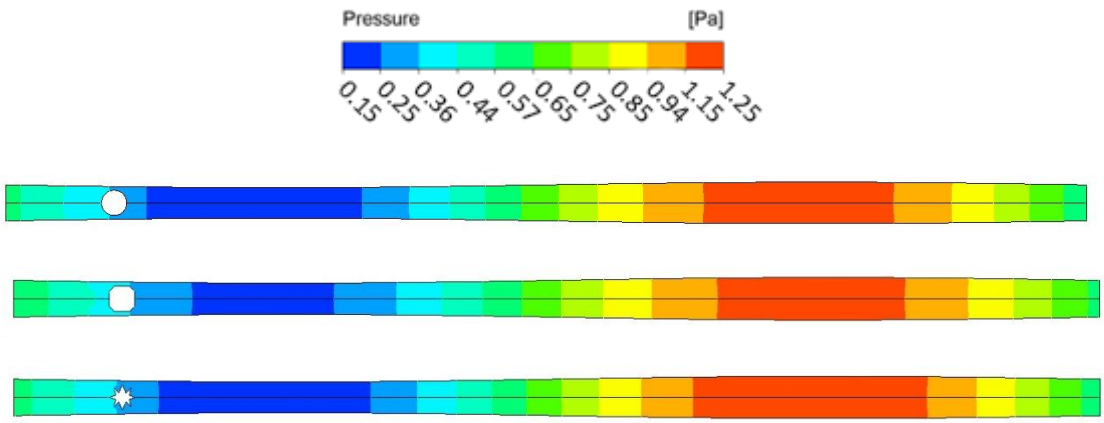

Figure 7: Pressure Contours for Various shapes of stone (round, hexagon and star)

various shapes, which replicate various real-life scenario. The contours for various blockages in ureter for pressure are displayed in Figure 7, for round, hexagonal and star shaped obstructions. Following the contraction wave, a high-pressure gradient is visible. The pressure gradient varies when the shape of stone is changed and noticeably greater for star shaped obstruction. Given that the volume hindrance remains constant at 70% for each form, the variations in the stone shapes can be accounted for the variations in velocities. For every scenario shown, the change in displacement per unit length vectors colored by the displacement per unit time magnitude in m/s were displayed at time when muscle contraction is at peak. Three distinct insets highlight and explain the flow patterns across the ureter in the presence of peristalsis muscle contraction wave. As the shape of the stone changes, the backflow proximal to the stone also increases. This could be because the hexagonal and star shaped

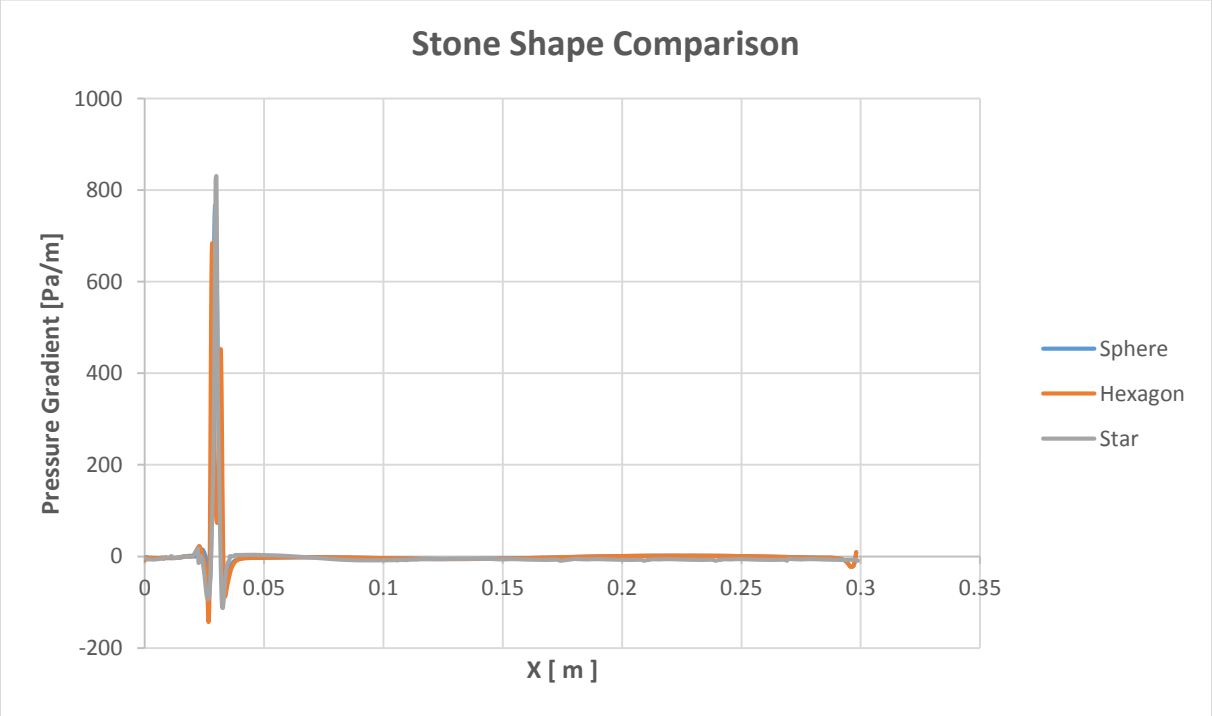

Figure 8: Comparison of Pressure Gradient for various shape stones (round, hexagon and star).

objects have more corners than round shaped stone, which increases recirculation in comparison This is due to an increase in the hydrostatic pressure near the obstruction can be also another reason and cause urine to

backflow. Because of the stone with more edges, the star shaped ureteral obstruction case had the greatest reverse velocities at the inlet and a substantial reverse flow at the start of ureter compared to all other scenarios. The round shaped stones have slightly lower velocities than the hexagonal and star-shaped stones, even if their distal velocity magnitudes are nearly similar. Zones with urine flow in reverse direction form in the various sections of the ureter as a result of the peristaltic action, and as edges of obstruction increases, the fluid velocities in the ureter distal to the stone decrease. For the ureter in each of the various obstruction scenarios, the magnitude of pressure gradient through the symmetry axis was examined and plotted. Here, the time instance of contraction is used to emphasise how the shape of the stone causes a difference in the effect. The magnitude of pressure gradient during the wall shrinkage under peristalsis are depicted in Figure 8. Pressure gradient "spikes" were caused by the stone's presence and peaked for star shaped stone scenario. As the edges of stone increased, these "spikes" increased. Thus, the smoothest stone had the lowest pressure gradient magnitude. More precisely, the round, hexagonal, and star-shaped stones have maximum pressure gradient magnitudes of 683.8 Pa/m, 766.1 Pa/m, and 830.3 Pa/m respectively. This is most likely due to the fact that as the edges of stone increases, the fluid becomes more obstructed, which lowers both the pressure within the obstruction and pressure change increases occurring across it.

Equation (4) was used to compute the magnitude of wall shear stresses in the presence of peristalsis wave of obstructed ureter. The results are displayed for the various obstructions in Figure 9. The stone shape has minimum effect on the behaviour of the wall shear stress. At the stone's placement, the wall shear stress increases noticeably before returning to its normal level. As the obstruction grows larger and edges are increased, the wall shear stress climbs to its peak value during contraction. This is fact due to the fluid fraction force increases as the obstruction volume increase. Thus, increasing the magnitude of wall shear stress and create high index pain.

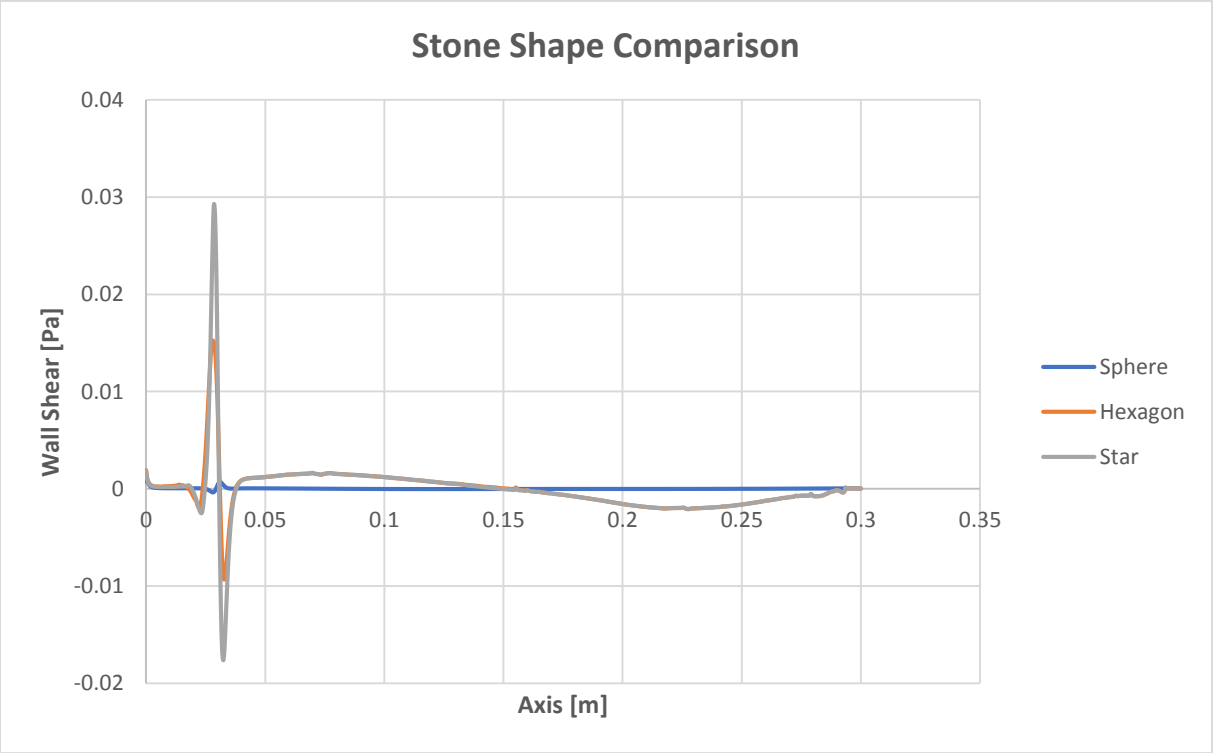

Figure 9: Comparison of Wall Shear Stress for various shape stones (round, hexagon and star).

IV. CONCLUSION

Using the industrial standard computational fluid dynamic code ANSYS FLUENT, two dimensional center line symmetric numerical modeling and simulations for urine flow in the normal and obstructed renal ureter were carried out in this study. A novel method for assessing the peristaltic process in the clogged ureter is shown by this simulation. It was investigated how different ureteral stone sizes affected peristalsis. More precisely, the wall contraction was found to be the cause of the reflux and trapping occurrences in the normal and obstructed ureter which was in line with previous investigations [15, 24, 27, 28]. The pressure gradient revealed higher pressures during contractions, which agreed with Hansen and Gregersen's data. According to

Hansen and Gregersen, the moment of contraction was when the peristaltic ureteral luminal pressure was at its highest. Lastly, backflow was seen at the ureter's entrance, which is in line with earlier research [13, 25]. The examination of urine flow in an obstructed ureter was the subject of the paper's subsequent section. A few research have examined the impact of muscle contraction mechanism peristalsis on tiny bits in the renal ureter [15, 18, 21, 27]. Still, a more thorough computational fluid dynamics analysis of the impact of blockage on backflow and ureter wall resistance per unit area in the renal ureter flows is still required. A preferable comprehension of the fluid flow in clogged renal ureters was obtained by inserting round stones into the ureter and analyzing the impact of the stone's increased size. Magnitude of backflow was found to be largest at the entrance for the highest 70 % obstruction case as the path of urine flow is almost clogged. Furthermore, increased pressure near stone causes the backflow of urine from ureter to renal pelvis and even into kidney collecting system. Backflow and separation of fluid layers near stone results in fluctuation of ureter wall shear stress. The increase in wall shear stress of ureter is also the result of stretching caused by the presence of kidney stone. The irregular shape and rough surface of kidney stone can also increase fluid friction against the ureter wall, thus increasing the wall shear stress. Those high fluid friction force can scratch the ureter wall and cause severe pain. There was a notable growth in the ureter wall resistance per unit area in the 70% blockage instance. Moreover, as urine is produced inside the kidney, hydrostatic pressure builds up and drives the urine from kidney towards the ureter. The presence of kidney stone resists the flow of urine and pressure drops occur. The largest stone (a 70% blockage) had larger pressure gradient magnitude values proximally and distally, and its obstruction-distant velocities were higher than those of the other obstructions.

The next part of research was focused on the effect of shape (hexagon and star shaped stone). The results revealed that kidney stone size has significant impact on urine flow compared to its shape. This can be due to the fact that for same size volume of obstruction is nearly same which can also be confirmed by results. The slight difference in magnitude of backflow for star and hexagon shaped stone is due to sharp edges. As the edges of stone are increased, it resist the flow of urine and lower the pressure of urine near stone. Similarly, low pressure gradient compared to other shapes is confirmed for round shaped stone due to its smooth surface. As the surface is smooth, fluid friction force is comparatively low and wall shear stress magnitude is low. These simulations along with studies of different stone shapes (round, hexagonal, star shaped) may improve our comprehension of how different stone shapes affect the ureteral wall and urine flow.

REFERENCE

[1]. Guyton AC, Hall JE. Urine formation by the kidneys: I. glomerular filtration, renal blood flow, and their control. Textbook of Medical Physiology; 1:309.

[2]. Drake R, Vogl AW, Mitchell AWM. Gray's Anatomy for Students, chap. 4. Philadelphia: Elsevier/Churchill Livingstone; 2005;326.

[3]. Bashir, A., Zuberi, S, K., Musharraf, B., (2022) "Perception of Dietary Influences on Renal Stone Formation Among the General Population" Cureus 14(6): e26024. doi:10.7759/cureus.26024

[4]. Prevalence of kidney stones in the USA: the National Health and Nutrition Evaluation Survey. Chen Z, Prosperi M, Bird VY. Journal of Clinical Urology. 2019;12:296–302.

[5]. Stone composition of renal stone formers from different global regions. Halinski A, Bhatti KH, Boeri L, et al. Arch Ital Urol Androl. 2021;93:307–312.

[6]. Liu SY, Lin JN, Huang CY, Tsai IT. Spontaneous rupture of the ureter mimicking acute appendicitis: two case reports. JACME. 2011;1(2):61-63.

[7]. Yin FC, Fung YC. Mechanical properties of isolated mammalian ureteral segments. Am J Physiol–Legacy Content. 1971;221(5):1484-1493.

[8]. Hansen I, Gregersen H. Morphometry and residual strain in porcine ureter. Scand J Urol Nephrol. 1999;33(1):10-16.

[9]. Sokolis DP. Multiaxial mechanical behaviour of the passive ureteral wall: Experimental study and mathematical characterisation. Computer Methods Biomech Biomed Engin. 2012;15(11):1145-1156.

[10]. Sokolis DP. Identification and characterisation of regional variations in the material properties of ureter according to microstructure. Computer Methods Biomech Biomed Engin. 2014;17(15):1653-1670.

[11]. Rassoli A, Shafigh M, Seddighi A, Seddighi A, Daneshparvar H, Fatouraee N. Biaxial mechanical properties of human ureter under tension. Urol J. 2014;11(3):1678-86.

[12]. Burns JC, Parkes T. 1967. Peristaltic motion. J Fluid Mech. 29:731–743.

[13]. Shapiro, A. H., Jaffrin, M. Y., and Weinberg, S. L., 1969, "Peristaltic Pumping With Long Wavelengths at Low Reynolds Number," J. Fluid Mech., 37(4), pp. 799–825.

[14]. Takabatake, S., and Ayukawa, K., 1982, "Numerical Study of Two-Dimensional Peristaltic Flows," J. Fluid Mech., 122, pp. 439–465.

[15]. Hung, T.-K., and Brown, T. D., 1976, "Solid-Particle Motion in Two-Dimensional Peristaltic Flows," J. Fluid Mech., 73(1), pp. 77–96.

[16]. Griffiths D. 1989. Flow of urine through the ureter: a collapsible, muscular tube undergoing peristalsis. Biomech Eng. 111(3):206–211.

[17]. Chrispell J, Fauci L. 2011. Peristaltic pumping of solid particles immersed in a viscoelastic fluid. Math Model Nat Phenomena. 6:67–83.

[18]. Jiménez-Lozano J, Sen M. 2010. Streamline topologies of twodimensional peristaltic flow and their bifurcations. Chem Eng Process. 49(7): 704–715. Process Intensification on Intensified Transport by Complex Geometries.

[19]. Zien TF, Ostrach S. 2015. A long wave approximation to peristaltic motion. J Biomech. 3(1):63–75.

[20]. Hosseini G, Williams JJ, Avital EJ, Munjiza A, Xu D, Green JA. Computational Simulation of Urinary System. San Francisco, USA: ProcWorld Congress Eng Comput Sci; 2012.

[21]. Chrispell J, Fauci L. Peristaltic pumping of solid particles immersed in a viscoelastic fluid. Math Model Nat Phenom. 2011;6(5):67-83.
[22]. Clavica F, Zhao X, ElMahdy M, Drake M, Zhang X, Carugo D. 2014. Investigating the flow dynamics in the obstructed and stented ureter by means of a biomimetic artificial model. PLoS One. 9(2):206–211.
[23]. Teran J, Fauci L, Shelley M. 2008. Peristaltic pumping and irreversibility of a stokesian viscoelastic fluid. Phys Fluids. 20(7):073101.
[24]. Vahidi B, Fatouraee N. 2012. A biomechanical simulation of ureteral flow during peristalsis using intraluminal morphometric data. J Theor Biol. 298:42–50.
[25]. Vahidi B, Fatouraee N. 2015. Mathematical modeling of the ureteral peristaltic flow with fluid structure interaction. J Biomech. 40:S223.
[26]. Vahidi B, Fatouraee N, Imanparast A, Moghadam AN. 2011. A mathematical simulation of the ureter: effects of the model parameters on ureteral pressure/flow relations. J Biomech Eng. 133(3):031004–031004.
[27]. Connington K, Kang Q, Viswanathan H, Abdel-Fattah A, Chen S. 2009. Peristaltic particle transport using the lattice boltzmann method. Phys Fluids. 21(5):053301.
[28]. Vahidi B, Fatouraee N, Imanparast A, Moghadam AN. 2011. A mathematical simulation of the ureter: effects of the model parameters on ureteral pressure/flow relations. J Biomech Eng. 133(3):031004–031004.
[29]. Hansen I, Gregersen H. 1999. Morphometry and residual strain in porcine ureter. Scand J Urology Nephrol. 33(1):10–16.